Multi Domain Mechatronic Optimization of an Intelligent Electro-Hydraulic Actuator

Dipl.-Ing. Dr. techn. Florian Poltschak

JKU HOERBIGER Research Institute for Smart Actuators (JHI), Johannes Kepler University Linz, Altenbergerstr. 69, 4040 Linz, E-Mail: florian.poltschak@jku.at

Dipl.-Ing. Oliver Koch

Institut für Fluidtechnik (IFD), Technische Universität Dresden, Helmholtzstr. 7a, 01069 Dresden, E-Mail: koch@ifd.mw.tu-dresden.de

Dr.-Ing. Babak Farrokhzad

Hoerbiger Automation Technology GmbH, Südliche Römerstr. 15, 86972 Altenstadt, E-Mail: babak.farrokhzad@hoerbiger.com

Professor Dipl. Ing. Dr. techn. Wolfgang Amrhein

Institute for Electrical Drives and Power Electronics, Johannes Kepler University Linz, Altenbergerstr. 69, 4040 Linz, E-Mail: wolfgang.amrhein@jku.at

Professor Dr.-Ing. Jürgen Weber

Institut für Fluidtechnik (IFD), Technische Universität Dresden, Helmholtzstr. 7a, 01069 Dresden, E-Mail: mailbox@ifd.mw.tu-dresden.de

Abstract

Electro-hydraulic systems combine the advantages of both, the electromagnetic and hydraulic domain and bring together e.g. the good controllability and precision of electrical drives as well as the unbeatable power density and higher robustness of hydraulics. An interesting application in this area is an electro-hydraulic actuator specifically designed for high-speed, high-force, high-precision punching applications. To further optimize the actuator design for the next machine generation the traditional layout process can be enhanced by an optimization step. This starts at the stage of conceptual design, needs a fundamental understanding of the underlying processes and a multi-domain mechatronic model. Therefore the simulation software designed for optimizing electrical machines is enhanced to cover electro-hydraulic and thermal issues too. The advantages of the integrated approach and the principle functionality of the simulation tool are demonstrated in context of the optimization of a newly developed electro-hydraulic actuator which was originally developed for punching machines.

KEYWORDS: multi-domain optimization, electro-hydraulic system, mechatronics

1. Introduction

Electro-hydraulic systems benefit from the combination of electric motors, actuators, sensors and control circuits as well hydraulic components. Objectives are for example a better or easier controllability with the use of an electronic control unit. Conventional systems for example take advantage of a speed control of pumps to optimize efficiency. These systems are mainly designed using standard components. The punching system that will be investigated here shows in addition a high degree of integration what redefines an electro-hydraulic system as a complex mechatronic system. A high power density combined with high dynamics is the benefit.

1.1. Linear punching system

The cross section of the punching actuator is given in **Figure 1 (a)** and shows the linear hydraulic direct drive (HDDL) which, mounted to a frame (e.g. a C-shaped frame), can perform punching, bending or pressing tasks. /1/

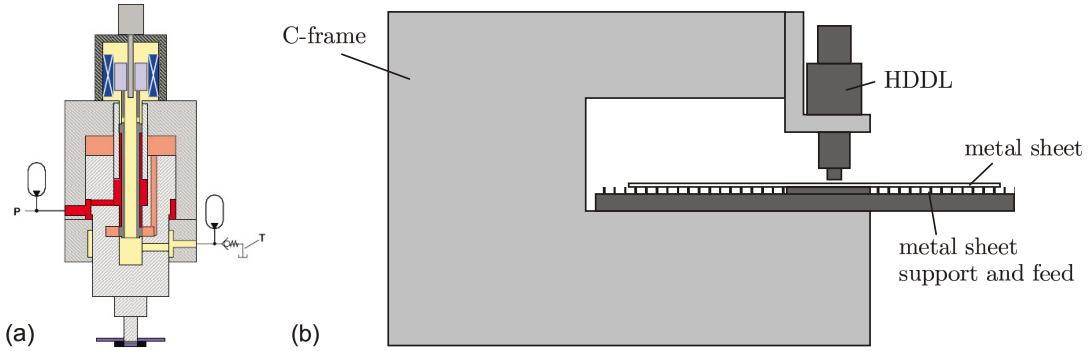

Figure 1: Hydraulic direct drive linear (HDDL) actuator

In contrast to the state of the art of actuators for punching machines, this actuator is characterized by the fact that the main components (valve, valve actuator and piston) only have a linear movement. This reduces the number of the components needed, resulting in higher reliability while increasing the actuator punching frequency and precision at the same time. The actuator features a linear motor which is directly connected to an integrated hydraulic spool valve taking advantage of a common bearing. Thus, the linear motor controls the hydraulic follower system. The electro-magnetic actuator is flooded with hydraulic oil and therefore thermally coupled to the hydraulic system. For reasons of versatility the actuator should have an optimum of output performance at a minimum of required space. The performance requirements range from high stroke rates to high positioning accuracy and form a challenging design task.

1.2. Requirements of customer applications

Though mainly designed for punching the HDDL-system can be used for applications ranging from punching to nibbling, marking, pressing, minting or bending and more. This versatility influences the performance requirements and leads to the definition of different load cycles. For example nibbling at high frequency and short stroke defines different demands for the electrical, mechanical, hydraulic and thermal layout as high precision pressing or even long stroke punching. This has to be taken into account when setting up the multi-domain model with suitable but different levels of detail.

Starting from the original prototype system the optimization objectives are to increase versatility in both: operation (e.g. higher stroke rates) and application (e.g. smaller overall size, lower costs). It is now the task of modelling to convert these objectives into objectives accessible for optimization.

2. Mechatronic modelling

Mechatronic modelling consists of an adequate combination of models from different disciplines. They are merged to meet the requirements of the optimization. In this case the objectives can be transferred to a minimization of power losses and armature mass (higher stroke rates) and a maximization of force density (smaller size, presumably lower material costs). On the other side the required acceleration of the spool can be influenced with the geometric dimensioning of the hydraulic system. This adds the objectives of a minimized required flow rate to minimize the size of the hydraulic power supply combined with a minimum required force at the spool to the optimization process. Hence the mechanic, electro-magnetic and hydraulic parts are interlinked making a multi domain optimization necessary. Despite these manifold connections between the domains not all of them need to be included in the optimization model. This results from the degree of influence of the connections on the optimization objective which is analyzed in /2/ using a model-based evaluation approach. The system boundary can therefore be defined as the boundaries of the HDDL-actuator. The link to the frame can be removed as all issues concerning vibrations are easier to solve optimizing the frame itself than the actuator because the origin rather lies within the high stroke frequency and the behaviour of the processed metal sheet than the actuator itself. With the movement of the actuator in air as the worst case in context of thermal and electromagnetic load, the application itself needs not be characterized in detail as it does not influence the optimization objectives in principle. Moreover the power electronics domain incorporates no optimization potential as a standard power electronics is used and therefore given as constraint.

For the given optimization objectives it is now necessary to consider and model the connections between the hydraulic, electro-magnetic and thermal domains. This can be further split up into two branches, one for the electro-magnetic-hydraulic link and one for the thermal link to the rest of the model. In this paper the thermal model is reduced to its minimum requirements represented by the maximum allowable power losses in the system. For this step of modelling the maximum allowable power loss is determined by experiment. Thus the thermal aspects merely serve as maximum limit for the optimization. A precise model of the thermal link will be subject of a prospective publication.

2.1. Electro-magnetic sub model

The electro-magnetic sub model consists of the linear motor to drive the spool valve and is embedded in hydraulic fluid. For reasons of compactness it uses the same bearing as the spool valve. As magnetic saturation cannot be neglected a Finite Element (FE) analysis with nonlinear material behaviour is necessary. Therefore the geometry is defined as a parametric model.

For the dynamic analysis the normalized voltage equation

$$\frac{\mathbf{u}(t)}{N} = R(\vartheta)\cdot\boldsymbol{\theta} + \frac{d\boldsymbol{\Psi}(x_s,\boldsymbol{\theta})}{dt} \tag{1}$$

can be applied with the number of windings N per phase, the ohmic resistance R and the vector of ampere turns $\boldsymbol{\theta}$, the flux vector $\boldsymbol{\Psi}$ and the position x_s of armature and spool. To include the boundary effects of the linear motor as well as saturation the dependencies of the flux $\boldsymbol{\Psi} = f(x_s, \boldsymbol{\theta})$ cannot be neglected. Using the flux linkage directly calculated in a FE analysis the equation can be transformed to

$$\boldsymbol{\Psi}(x_s,\boldsymbol{\theta}) = \int\left(\frac{\mathbf{u}(t)}{N} - R(\vartheta)\cdot\boldsymbol{\theta}\right)dt \tag{2}$$

With the voltage $\boldsymbol{u}$ as input vector the function $\boldsymbol{\theta} = f(x_s, \boldsymbol{\Psi})$ is needed, which is an inverse function to the calculated expression $\boldsymbol{\Psi} = f(x_s, \boldsymbol{\theta})$. The inversion is only possible if $\boldsymbol{\Psi}$ is strictly monotonous in $\boldsymbol{\theta}$. Furthermore the three phase system has only two degrees of freedom for a given connection, which is a star connection in this case. Hence the system needs to be transferred to a two degree of freedom representation instead of a direct three phase modelling. The first step is to transfer the linear system to a rotational coordinate system to be able to use trigonometric transformations. Using the relation

$$x_s = \frac{\tau_p}{\pi}\varphi \tag{3}$$

the linear coordinate x_s can be transformed to the rotational angle φ with the pole pitch τ_p. This is only valid if the boundary effects of a linear motor can be neglected, which has to be checked for the given system. However it allows the use of a Fourier series representation what simplifies calculations. Applying the Park/Clarke transform with the transformation matrix

$$\mathbf{M}(\varphi) = \frac{2}{3}\begin{bmatrix} \cos(\varphi) & \cos(\varphi - 2\pi/3) & \cos(\varphi - 4\pi/3) \\ -\sin(\varphi) & -\sin(\varphi - 2\pi/3) & -\sin(\varphi - 4\pi/3) \\ 1/2 & 1/2 & 1/2 \end{bmatrix} \tag{4}$$

the three phase system is transformed to the armature oriented coordinate system d/q. Hence the vectors of flux, voltage or ampere turns

$$\begin{bmatrix} \theta_d & \theta_q & \theta_0 \end{bmatrix}^T = M(\varphi)\begin{bmatrix} \theta_a & \theta_b & \theta_c \end{bmatrix}^T \tag{5}$$

can be directly transformed. As the function $\boldsymbol{\theta} = f(x_s, \boldsymbol{\Psi})$ is now needed in d/q representation the FE analysis can directly be used to calculated the transformed table $\boldsymbol{\Psi}_{dq} = f(x_s, \boldsymbol{\theta}_{dq})$ with respect to the transformed d/q coordinate system. The phase representation is derived by pre-multiplication of the inverse matrix of **M**. Finally the inversion of the table $\boldsymbol{\Psi}_{dq}$ lead to the table $\boldsymbol{\theta}_{dq} = f(x_s, \boldsymbol{\Psi}_{dq})$. The transformation of the equation (2) leads to the system

$$\boldsymbol{\Psi}_{dq}(x_s, \boldsymbol{\theta}_{dq}) = \int \left(\frac{\mathbf{u}_{dq}(t) - \mathbf{u}_{emf,dq}}{N} - R(\vartheta) \cdot \boldsymbol{\theta}_{dq} \right) dt \tag{6}$$

with the induced voltage $\mathbf{u}_{emf,dq}$ resulting from the transformation.

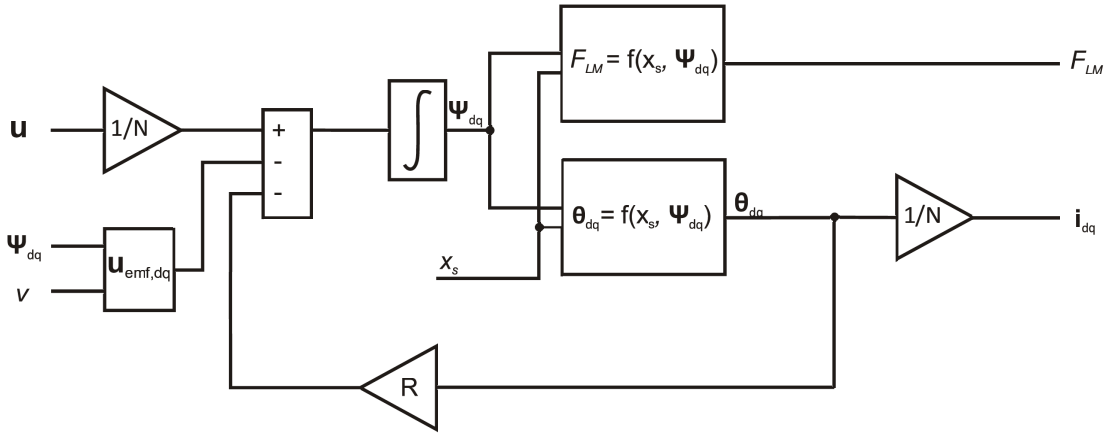

Figure 2: Structure of the dynamic electro-magnetic sub system

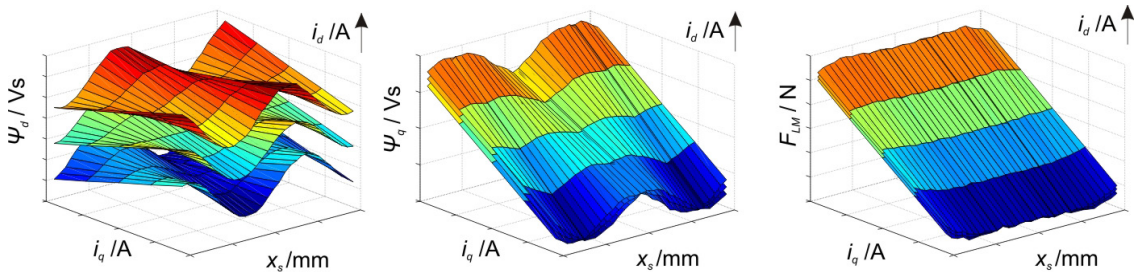

Figure 3: FEM based representation of the linear drive

As second result from the FE analysis the derived force $F_{LM} = f(x_s, \boldsymbol{\theta}_{dq})$ of the linear motor can be transformed to the representation $F_{LM} = f(x_s, \boldsymbol{\Psi}_{dq})$ completing the model structure given in **Figure 2**. The model is validated by measurement in both: steady-state and dynamic operation. **Figure 3** shows the tables resulting from the FE analysis and used in the model in Figure 3.

2.2. Hydraulic sub model

The following section describes how to model the drive's hydraulics and mechanics. **Figure 4** shows an abstract description of the subsystem. The model consists of basic hydraulic components (volume, orifice, throttle and inductance) which were parameterized based on their geometry.

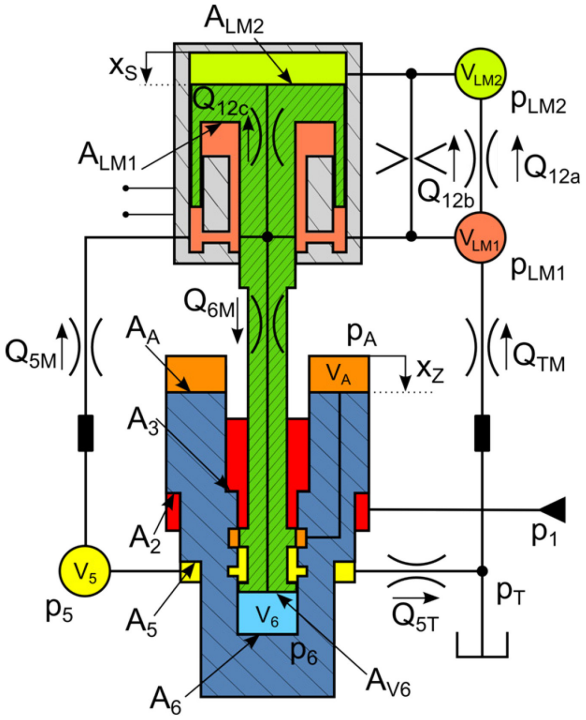

Figure 4: Structure of the hydraulic sub model.

The follower system operates like a control loop. The valve spool dictates the set position and thus changes the system's static equilibrium. A force acts on the cylinder

which causes a change in its position until the equilibrium is recovered. The valve spool is positioned almost load-free. Amplified by the hydraulics, the cylinder follows the valve. A force-path relation connects the electro-magnetic and the hydraulic-mechanical subsystem. While the motor force information is passed to the hydraulic subsystem the electro-magnetic model receives the valve position.

The displacement volume V_A is connected to the system pressure p_1 or via bore Q_{5T} to the tank pressure p_T depending on the spool valve's position. It is assumed that the pressure level of the system pressure p_1 and the tank pressure p_T are constant. The equation for the cylinder motion in direction x_z is given by

$$A_A \cdot p_A + (A_3 - A_2) \cdot p_1 + A_6 \cdot p_6 - A_5 \cdot p_5 = m_Z \cdot \ddot{x}_Z + b_Z \cdot \dot{x}_Z + F_{friction} + F_{load} \qquad (7)$$

with the areas A_i and their corresponding pressures p_i, the mass of the cylinder m_z, the damping coefficient b_s, the friction force $F_{friction}$ and the load force F_{load}. With the defined boundary conditions and a constant load, the pressure p_A influences the cylinder motion significantly. Compared to the force $F_A = p_A A_A$ the forces $F_5 = p_5 A_5$ and $F_6 = p_6 A_6$ are negligibly small.

The linear motor positions the valve spool. It is mounted in oil and its oil chamber is connected to the tank via two bores. The purpose of both bores is to cool the motor. Bore Q_{5M} connects the volume V_5 and the linear motor. The second bore connects the linear motor and the tank p_T. Due to the high dynamic stress and the length of the bores, the inductive behavior of oil column has to be modeled as well. The throttles Q_{12c} and Q_{6M} represent the oil exchange between volumes connected by the spool bore. Throttle Q_{12a} stands for the gap between the housing and the winding of the linear motor. The notches in the motor are modeled as orifice Q_{12b}. Compared to the other resistances the geometrical length of orifice Q_{12b} is very small in relation to its flow cross section. Disregarding the friction, the equation of the valve spool movement in direction x_s is given by

$$A_{LM2} \cdot p_{LM2} - A_{LM1} \cdot p_{LM1} - A_{V6} \cdot p_6 + F_{LM} - F_{flow} = m_S \cdot \ddot{x}_S \qquad (8)$$

where the index LM stand for 'linear motor'. **Figure 5** shows a simulation result. The relative position $y = x_S - x_Z$ between valve spool and cylinder defines the cross section of the control edge. A positive change of the valve spool's position from its steady state position opens the control edge p_1-p_A. Due to the pressure difference a volume flow leads to a pressure increase in the displacement volume V_A. The altered force balance results in a positive cylinder movement. Changing the position of the valve spool from

its equilibrium in negative direction opens the control edge p_A-p_T which entails a drop in pressure in the displacement volume V_A. The cylinder accelerates in negative direction.

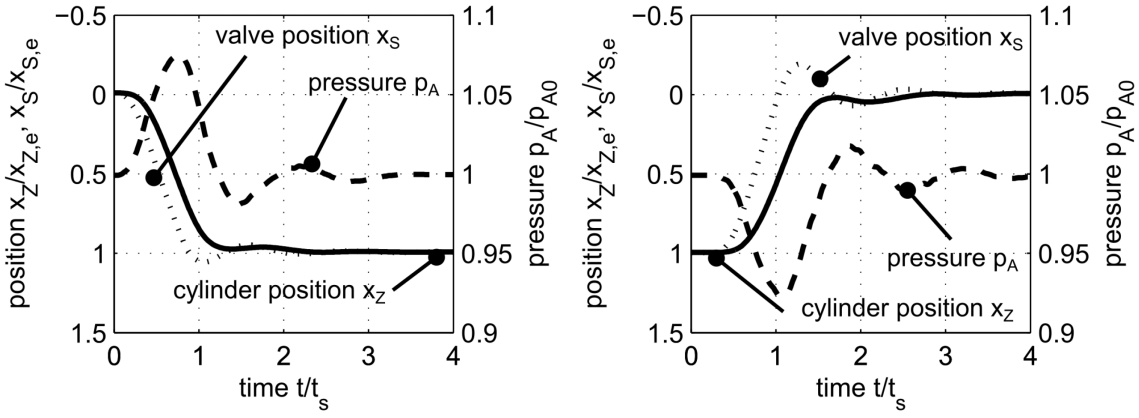

Figure 5: Simulation result

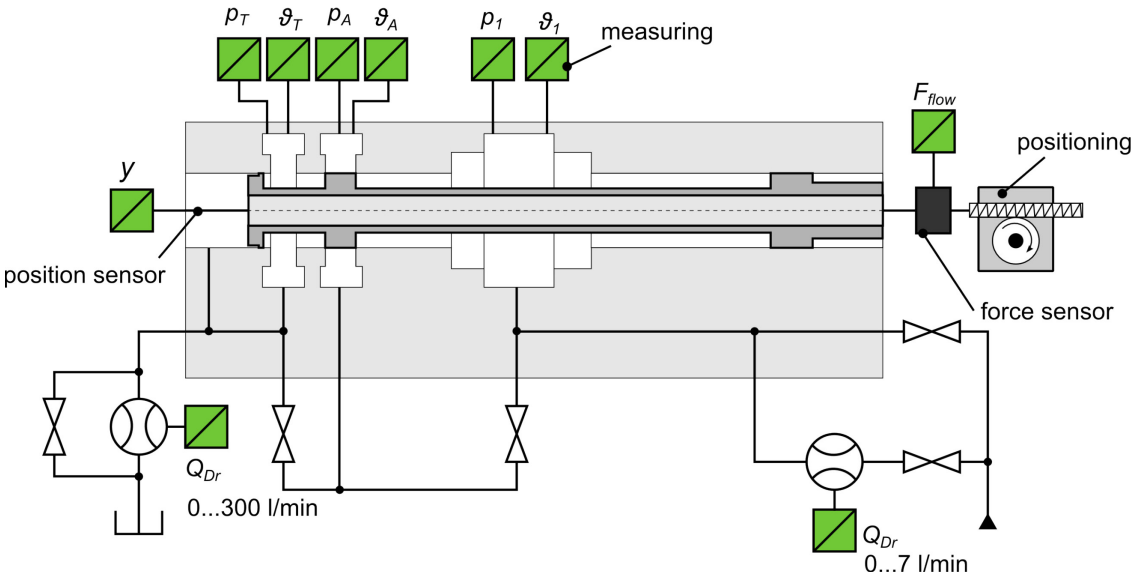

Figure 6: Principle structure

Not all parameters for the simulation model can be concluded from engineering drawings. Thus, a test setup was built to examine the processes at the control edge in more detail. **Figure 6** shows the principle structure. The valve spool and its entire control edge geometry are located in a special-design valve block which connects the hydraulic supply and all necessary sensors. A spindle is used to position the valve spool exactly and thus to control the cross section of the control edge. For different valve spool positions the pressure difference is varied and the volume flow is measured. The resulting pressure-volume flow-stroke-characteristic is shown in **figure 7a**. Figure 7b shows the measured flow force versus the volume flow and the

valve spool position. Based on these measurements the flow rate characteristic of the control edge and the flow force were implemented into the simulation model.

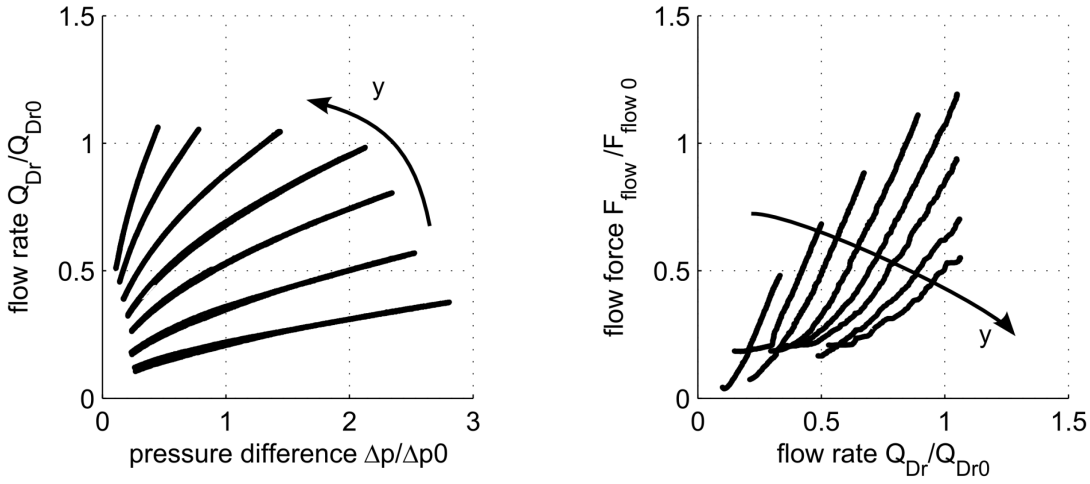

Figure 7: Measurement results

3. Multi-domain optimization

The mathematical models described above are implemented and integrated in the multi-domain optimization tool MagOpt. The first step is to parameterize the geometry of the electro-magnetic and hydraulic part. Many potential parameters for optimization can be identified. Though there is no restriction of number in context of the optimization algorithm or mathematical modelling it is advisable only to use a limited number of the parameters with the biggest impact on the optimization objectives.

The parameters selected for the optimization are:

- The geometric dimensions of the linear drive with focus on the armature (including the directly connected spool).
- The dimensions of the hydraulic circuit with focus on the cylinder diameters.

The selected objectives are:

- Actuator force: A maximum actuator force per volume reduces overall size.
- Weight of moved parts: Less weight increases the dynamics. This is especially important for the moved mass of the linear motor and therefore the dynamics of the spool. On the other hand a reduced size of the armature reduces forces and therefore dynamics.
- Power losses: Reduced losses expand the field of possible further applications.

- Hydraulic power supply and optimal utilization of the linear drive: The dimensioning of the cylinder defines the size of the needed hydraulic power supply and the dynamic requirements of the linear drive. This opposes an energy efficient use of the linear drive.

It can be clearly seen that the selected objectives are in some points contradictory whereas their influence on further objectives cannot be simply identified. Here a multi-domain optimization shows its strength. The calculation of the Pareto front gives all optimal solution without the need of weighting the objectives before the optimization is done.

Each solution on the Pareto front is an optimum to all given objectives. Any further changes of parameters deteriorate the solution within at least one objective. Thus one of the Pareto solutions can be directly selected according to the final weighting of the optimization objectives. The results in **Figure 8** and **9** are plotted relative to the prototype system used to validate the models. Figure 8 (a) gives the linear motor force and Figure 8 (b) the maximum acceleration in relation to the spool and armature mass and the power losses (heat source) in the linear drive. The result shows that the mass of spool and armature can even be increased while keeping the maximum achievable acceleration and the power losses equal. Next to this the power losses of the linear motor can further be reduced by optimizing the size of the areas in the equations 7 and 8 in order to maximize the utilization of the linear motor as shown in Figure 9 (b). Figure 9 (a) gives the relation of the required spool force to the volume flow (required power) of the installed hydraulic pump. Dependent on the application (load force) the system can be designed to minimize the power consumption of the hydraulic pump without reducing the performance (acceleration).

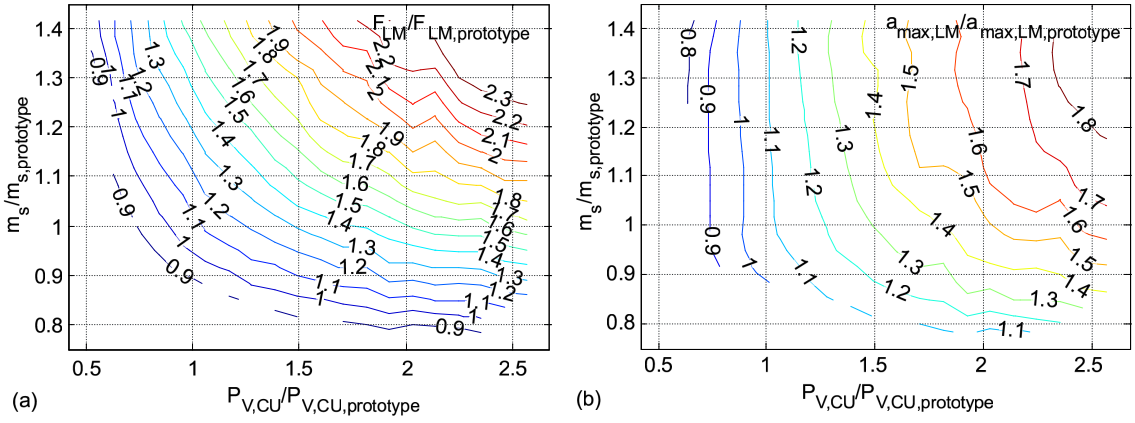

Figure 8: Surface of the Pareto optimum of the (a) force F_{LM} of the linear motor and (b) the maximum possible acceleration $a_{max,LM}$.

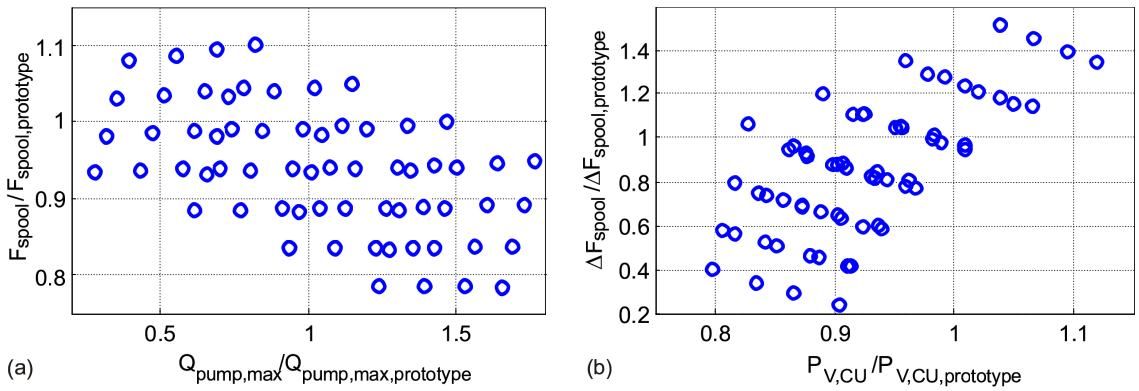

Figure 9: Relationship between hydraulic and electromagnetic objectives due to variation of hydraulic cross sections.

4. Conclusion

The highly integrated structure of the electro-hydraulic actuator makes a multi-domain modelling necessary. Identifying the touched domains different levels of detail can be applied to different domains according to their connection to the specified optimization objectives. As the actuator finds its application in tool machines the specific use case has a major influence on the optimal performance. To solve this issue the objectives of the optimization process are selected to be independent of the final application as far as possible. Hence the model concentrates on the electro-magnetic and hydraulic domains. Both subsystems are parameterized and combined in a co-simulation including the FE analysis of the electro-magnetic circuit and the dynamic simulation of the whole system. Finally the Pareto optimum is calculated for the identified objectives using the optimization tool MagOpt.

The results show the optimization potential of the system. In combination with the boundary condition of a specific application which defines amongst others the thermal limit and therefore the maximum acceptable losses a specific optimum can be selected.

Literature

/1/ Ritzl J. & Kurz M. 2010. Hybridantrieb sorgt für Dynamik und Präzision bei Stanzmaschinen, MM Maschinenmarkt. pp. 44–46.

/2/ Poltschak F., Hehenberger P., Farrokhzad B., Amrhein W. & Zeman K. 2011. Model-based Evaluation of a Linear Electro Hydraulic Direct Drive, EUROCAST 2011, Feb 6-11 2011, 13th International Conference on Computer Aided Systems Theory, Las Palmas, Gran Canaria, Spain

Nomenclature

u	voltage	V
N	Number of windings of a phase	-
ϑ	temperature	K
R	ohmic resistance	Ω
$\boldsymbol{\theta}$	vector of ampere turns	A
$\boldsymbol{\Psi}$	vector of flux	Vs
x_s	position of spool-armature assembly	mm
x_z	position of cylinder	mm
t	time	s
φ	rotational angle	rad
τ_p	pole pitch	-
$\mathbf{M}$	Park/Clarke transformation matrix	-
A_i	Area	mm^2
p_i	Pressure acting on area x	Pa
F_i	force	N
Q_i	flow rate	l/min
m_i	mass of body i	kg
V_i	Volume i	mm^3
b_i	damping coefficient	Ns/m
y	relative distance between spool and cylinder	mm